



Pergamon

Energy 25 (2000) 427–443

ENERGY

www.elsevier.com/locate/energy

A risk based heat exchanger analysis subject to fouling Part I: Performance evaluation

Syed M. Zubair^{*}, Anwar K. Sheikh, Muhammad Younas, M.O. Budair

Department of Mechanical Engineering, King Fahd University of Petroleum & Minerals, Dhahran 31261, Saudi Arabia

Abstract

Heat exchangers operating in the power and process industries are fouled to a greater or lesser extent depending on surface temperature, surface condition, material of construction, fluid velocity, flow geometry and fluid composition. This fouling phenomenon is time-dependent and will result in a decrease in the thermal effectiveness of a heat exchanger. Once the thermal effectiveness decreases to a minimum acceptable level, cleaning of the equipment becomes necessary to restore the performance. In this paper, we present a simple probabilistic approach to characterize various fouling models that are commonly encountered in many industrial processes. These random fouling growth models are then used to investigate the impact on risk-based thermal effectiveness, overall heat-transfer coefficient and the hot- and cold-fluid outlet temperatures of a shell-and-tube heat exchanger. All the results are presented in a generalized form in order to demonstrate the generality of the risk-based procedure discussed in this paper. © 2000 Elsevier Science Ltd. All rights reserved.

1. Introduction

Heat exchangers are extensively used in the power and process industries to transfer heat from one fluid stream to another. The thermal–hydraulic performance of these heat exchangers decreases continuously with time due to fouling, which is defined as the formation of deposits on heat transfer equipment (HTE). These deposits may be due to sedimentation, crystallization, organic or biological growths, corrosion products, or a combination of these effects [1–5]. In addition, where the heat flux is relatively high, as in steam generators, fouling can lead to local hot spots and ultimately may result in mechanical failure of HTE, and hence an unscheduled shutdown of the plant. This may result in both economic and human loss, particularly in refineries and thermal power plants. It is also important to mention that the designers and operators of HTE

^{*} Corresponding author. Tel.: +966-3-860-2540; fax: 966-3-860-2949.
E-mail address: smzubair@kfupm.edu.sa (S.M. Zubair).

Nomenclature

A	heat transfer area (m^2)
\dot{C}	fluid capacitance rate (W K^{-1})
C_r	fluid capacitance ratio ($C_r = \dot{C}_{\min} / \dot{C}_{\max}$)
f	probability density function (h^{-1})
HTE	heat transfer equipment
ΔH	enthalpy change (J)
M	median time (h)
\dot{m}	mass flow rate (kg h^{-1})
n	number of shell passes
NTU	number of transfer units ($NTU = UA / \dot{C}_{\min}$)
P	probability
p	risk level
\dot{Q}	heat transfer rate (W)
R_f	fouling resistance ($\text{m}^2 \text{K W}^{-1}$)
$R_{f,c}$	critical fouling resistance ($\text{m}^2 \text{K W}^{-1}$)
T	temperature (K)
t	time (h)
t_c	time constant (h^{-1})
U	overall heat-transfer coefficient ($\text{W m}^{-2} \text{K}^{-1}$)

Greek symbols

$\sqrt{\alpha}$	scatter in time
ε	heat exchanger effectiveness
$\Phi()$	cumulative normal distribution function
ϕ	rate of deposition or removal ($\text{m}^2 \text{K J}^{-1}$)

Subscripts

C	clean condition
c	cold fluid
c,i	cold-fluid inlet
c,o	cold-fluid outlet
d	deposition
F	fouled condition
f	fouling
h	hot fluid
h,i	hot-fluid inlet
h,o	hot-fluid outlet

max	maximum
min	minimum
r	removal

Superscripts

*	asymptotic value
<i>n</i>	exponent for the power-law model

must be able to predict performance variations as the fouling proceeds. The designer needs this information to ensure that the user requirements with regard to preventive maintenance schedules can be met, while the user of HTE must be able to formulate rational operating schedules for equipment-management purposes.

To answer some of the questions of the designers and operators of HTE, a project is being carried out at the King Fahd University of Petroleum and Minerals, Dhahran. One of the major objectives of the project is to provide a risk-based mathematical structure to the heat exchanger fouling problem and then discuss rational maintenance and/or replacement strategies to reduce the overall maintenance and operating costs of heat exchangers subject to fouling. In this paper, we present a risk-based (or probabilistic) approach to the analysis of fouling models and then describe its impact on the thermal performance of heat exchangers.

2. Fouling growth models

The most widely accepted fouling model is based on the following general material balance equation first proposed by Kern and Seaton [6]:

$$\frac{dR_f(t)}{dt} = \phi_d - \phi_r \quad (1)$$

It should be noted that the rate of fouling deposition, ϕ_d , depends on the type of fouling mechanism (sedimentation, crystallization, organic material growth, etc.), while the rate of fouling removal, ϕ_r , depends on both the hardness or adhesive strength of the deposit and the shear stress due to the flow velocity, as well as the system configuration. The rates of deposition and removal have been given many different forms (depending upon the type and mechanism of fouling) by various investigators. This time-dependent behavior of the fouling process can be characterized by a number of fouling models proposed in the literature [1,2,5–8]. These models are the linear, power-law, falling-rate and asymptotic fouling growth models and are discussed by Zubair et al. [9,10] and Sheikh et al. [11]. The different models result from the large number of uncertainties associated with the fouling growth process, particularly when considering actual heat exchanger applications. Zubair et al. [9,10] and Sheikh et al. [11] have demonstrated that these models are probabilistic in nature. In particular, the distribution of fouling resistance of heat exchanger tubes with respect to time characterizes these random processes. They have shown that there is a considerable

scatter in $R_f(t)$ at any time t and, similarly, for any fixed value of R_f , there is a corresponding scatter in the values of t . Sheikh et al. [11] have also demonstrated that for a fixed risk level $p=P(R_f(t)\leq R_{f,c})$, where $R_{f,c}$ is the critical acceptable value of fouling resistance, the time to reach this critical value will be distributed as an alpha distribution for a linear fouling growth model, i.e., when $R_f(t)$ is a linear function of time. It is important to mention that the probability distribution function has two main indicators, namely the median time, M , to reach the critical level of fouling [i.e., $p=0.50=P(R_f(t)\leq R_{f,c})$] and a scatter in the growth rate of the fouling process described by a scatter parameter $\sqrt{\alpha}$. As will be demonstrated in the following sections, these two parameters have a significant impact on the thermal performance of heat exchangers.

2.1. Linear fouling model

Linear fouling behavior is generally associated with the crystallization of a well-formed deposit consisting of a substantially pure salt that is largely uncontaminated by the presence of co-precipitated impurities. The strong bonds characterizing the structure of such deposits prevent significant removal rates. This hypothesis, initially proposed by Taborck et al. [1], was further supported by the experimental work of Hasson et al. [12], Andritsos et al. [13] and Zubair et al. [14] while investigating the mechanism of CaCO_3 scale growth in laboratory experiments.

In this regard, a random linear fouling growth model for the case when the critical acceptable value of fouling resistance $R_{f,c}$ is given can be expressed in terms of risk level p and scatter parameter $\sqrt{\alpha}$ as

$$R_f(t, p; \sqrt{\alpha}) = R_{f,c}(t/t_{p,c}) = R_{f,c}[1 - \sqrt{\alpha}\Phi^{-1}(p)](t/M). \tag{2}$$

Fig. 1 shows the representation of Eq. (2) in terms of reduced time t/M and risk level p for a

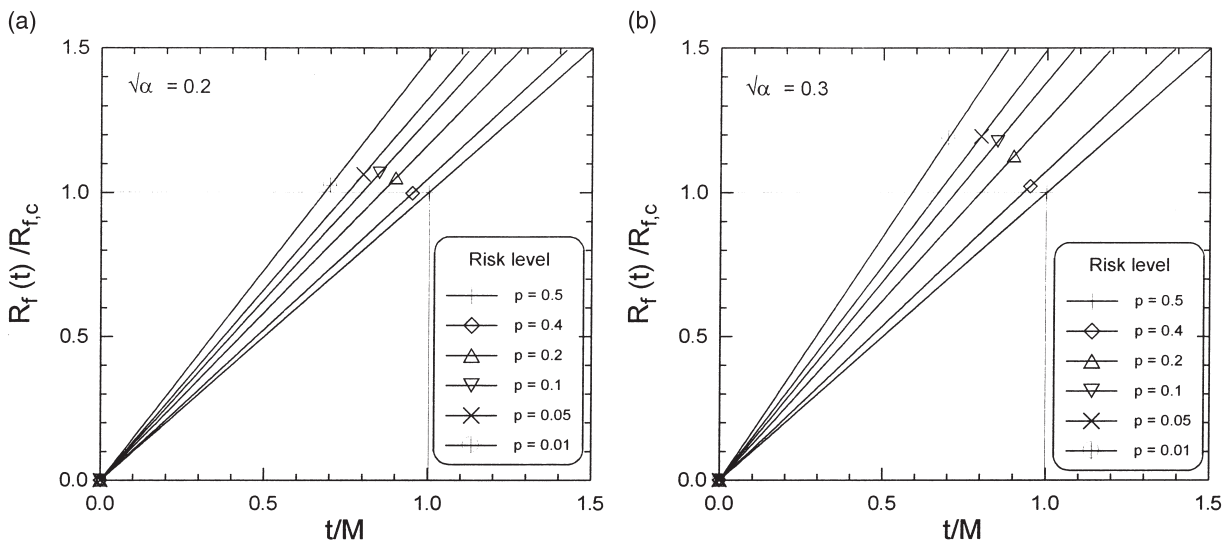


Fig. 1. Reduced random fouling resistance versus reduced time for a linear model with different values of risk level p and scatter parameter: (a) $\sqrt{\alpha}=0.20$; and (b) $\sqrt{\alpha}=0.30$.

given scatter parameter $\sqrt{\alpha}$. Fig. 1(a) is for $\sqrt{\alpha}=0.20$, while Fig. 1(b) is for $\sqrt{\alpha}=0.30$. It can be seen from these figures that for a low risk level, for example when $p=0.01$ (i.e., 99% reliability), the time to reach the critical level of fouling is much smaller than for the deterministic case (i.e., $p=0.50$). As expected, Fig. 1(b) shows somewhat more scatter and that an even smaller time is required to reach the critical value at a given risk level compared with Fig. 1(a).

2.2. Power-law fouling model

The power-law fouling growth mechanism has been observed by Khan et al. [15] while investigating the deposition of CaCO_3 under relatively high operating temperatures. Sheikh et al. [11] have also shown that replicate corrosion fouling data of Somerscales and Kassemi [16] can be represented by a power-law model.

A random version of the power-law fouling growth model on a linearly transformed time scale can be expressed similarly to the linear fouling model as

$$R_f(t, p; \sqrt{\alpha}) = R_{f,c}(t/t_{p,c})^n = R_{f,c}[1 - \sqrt{\alpha}\Phi^{-1}(p)]t^n/M^n, \tag{3}$$

where the risk-based time to reach the critical fouling resistance for the power-law model is expressed as

$$t_{p,c} = M/[1 - \sqrt{\alpha}\Phi^{-1}(p)]^{1/n}. \tag{4}$$

It is important to mention that M and $\sqrt{\alpha}$ represent the median time and the scatter parameter, respectively, in a transformed coordinate system where the power-law model is treated as a linear model.

Fig. 2 illustrates the fouling resistance as a function of reduced time t/M and the risk level p

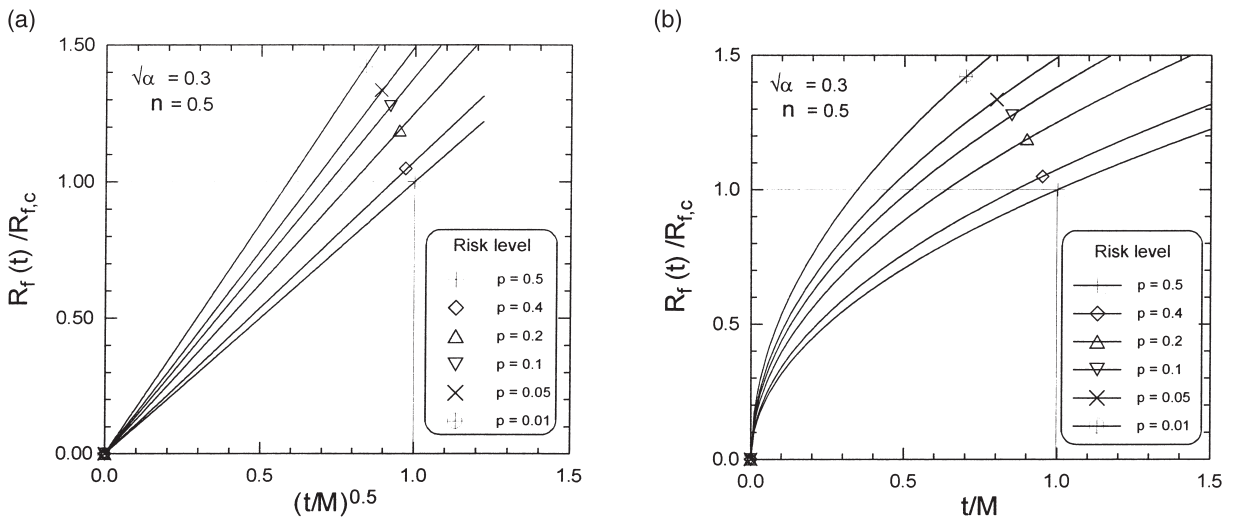


Fig. 2. Reduced random fouling resistance versus reduced time for a power-law model with different values of risk level p , scatter parameter $\sqrt{\alpha}=0.30$ and power of the exponent $n=0.50$: (a) in a transformed x -axis; (b) in a non-transformed x -axis.

for the scatter parameter $\sqrt{\alpha}=0.30$. In plotting this figure, the exponent for the power-law model is taken as $n=0.50$, which is representative of corrosion fouling data presented in Ref. [16]. As expected, this figure also shows that, for a low risk level, the time to reach the critical level of fouling is much smaller than for the deterministic case (i.e., $p=0.50$). On comparing Fig. 2(a) with Fig. 2(b), we note that the scatter in the growth rate in the transformed coordinate system is different from that in the non-transformed coordinate system.

2.3. Falling-rate fouling model

Falling-rate fouling normally occurs in situations where the deposition rate is always greater than the removal rate. This type of fouling mechanism has been observed by Muller-Steinhagen et al. [17] while investigating the influence of operating conditions on particulate fouling. In addition, the data of Bansal and Muller-Steinhagen [18] for crystallization fouling in a plate exchanger also show a falling-rate trend. It should be noted that random falling-rate fouling data on a linearly transformed time scale could be expressed in a manner similar to that of the power-law model as

$$R_f(t, p; \sqrt{\alpha}) = R_{f,c}[\ln(t)/\ln(t_{p,c})] = R_{f,c}[1 - \sqrt{\alpha}\Phi^{-1}(p)]\ln(t)/\ln(M). \tag{5}$$

Here, also similar to the power law model, the parameters M and $\sqrt{\alpha}$ represent the median time and the scatter parameter in a linearly transformed coordinate system, where the falling-rate model is treated as a linear model. In this regard, the risk-based time for the falling-rate model is expressed as

$$\ln(t_{p,c}) = \ln(M) / [1 - \sqrt{\alpha}\Phi^{-1}(p)]. \tag{6}$$

Fig. 3 shows the plot of reduced fouling resistance $R_f(t)/R_{f,c}$ as a function of reduced time t/M

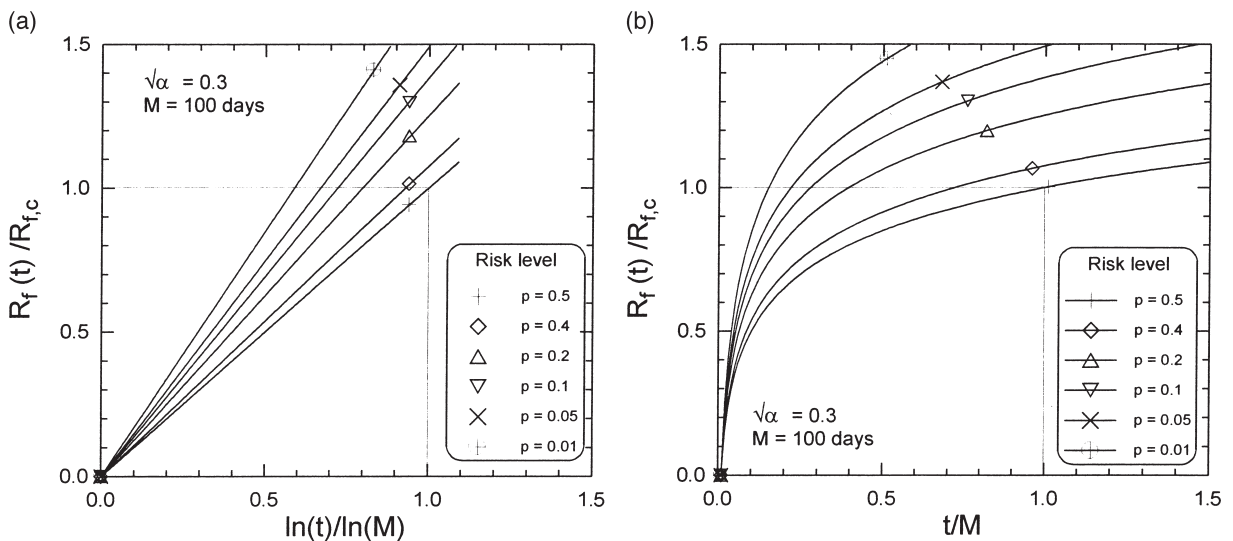


Fig. 3. Reduced random fouling resistance versus reduced time for a falling-rate model with different values of risk level p and scatter parameter $\sqrt{\alpha}=0.30$: (a) in a transformed x -axis; (b) in a non-transformed x -axis.

and risk level p for the scatter parameter $\sqrt{\alpha}=0.30$. In this figure we note again that the scatter in the fouling growth rate in the transformed coordinate system is different from that in the non-transformed coordinate system. Also, we notice that the time to reach the critical level of fouling is large for a deterministic case ($p=0.50$) compared with a low risk level case. For example, the reduced time to reach the critical level for $p=0.10$ (i.e., 90% reliability) is about 30% that of the deterministic case.

2.4. Asymptotic fouling model

An asymptotic fouling growth model is often observed in cooling water heat exchangers. In these heat exchangers, the conditions leading to the formation of a scale layer of a weak, less coherent structure are associated with the simultaneous crystallization of salts of different crystal shapes, or with the presence of suspended particles embedded in the crystalline structure. Hasson [19] has indicated that growth of such deposits is expected to create internal stresses in the scale layer, so that the removal processes become progressively more effective with the deposit thickness. Such considerations lead to an asymptotic scale thickness, at which the deposition is balanced by the scale removal mechanism.

The random (or probabilistic) asymptotic fouling growth model on a transformed y -axis can be written as

$$\ln[1/(1-R_f/R_f^*)]=t/t_C. \quad (7)$$

The above equation may be explained as a linear version of the asymptotic fouling growth model, where the time constant t_C is expressed in terms of the critical acceptable value of fouling resistance $R_{f,c}$ and the time to reach this critical value $t_{p,c}$, expressed as

$$t_C=t_{p,c}/\ln[1/(1-R_{f,c}/R_f^*)] \quad (8)$$

and

$$t_{p,c}=M/[1-\sqrt{\alpha}\Phi^{-1}(p)]. \quad (9)$$

Substituting the value of t_C into Eq. (7) and rearranging, we get

$$R_f(t, p; \sqrt{\alpha})=R_f^*[1-\exp\{-\ln[1/(1-R_{f,c}/R_f^*)][1-\sqrt{\alpha}\Phi^{-1}(p)]t/M\}]. \quad (10)$$

Similar to the above two random fouling growth models, the parameters M and $\sqrt{\alpha}$ represent the median time and the scatter parameter in a transformed coordinate system, where the exponential fouling growth model may be treated as a linear model.

Fig. 4 shows the plot of fouling resistance as a function of reduced time t/M and the risk level p for the scatter parameter $\sqrt{\alpha}=0.30$. It should be noted that, in plotting this figure, we have considered the critical fouling resistance as 95% that of the asymptotic value. This critical value may be considered as a representative number for most cooling water heat exchangers when it becomes necessary to clean the exchanger. As expected, this figure also shows that, for a low risk level, the time to reach the critical level of fouling is faster than in the deterministic case (i.e., $p=0.50$). Again, we notice in this figure that the scatter in the growth rate is much different in the transformed coordinate system when compared with the non-transformed coordinate system.

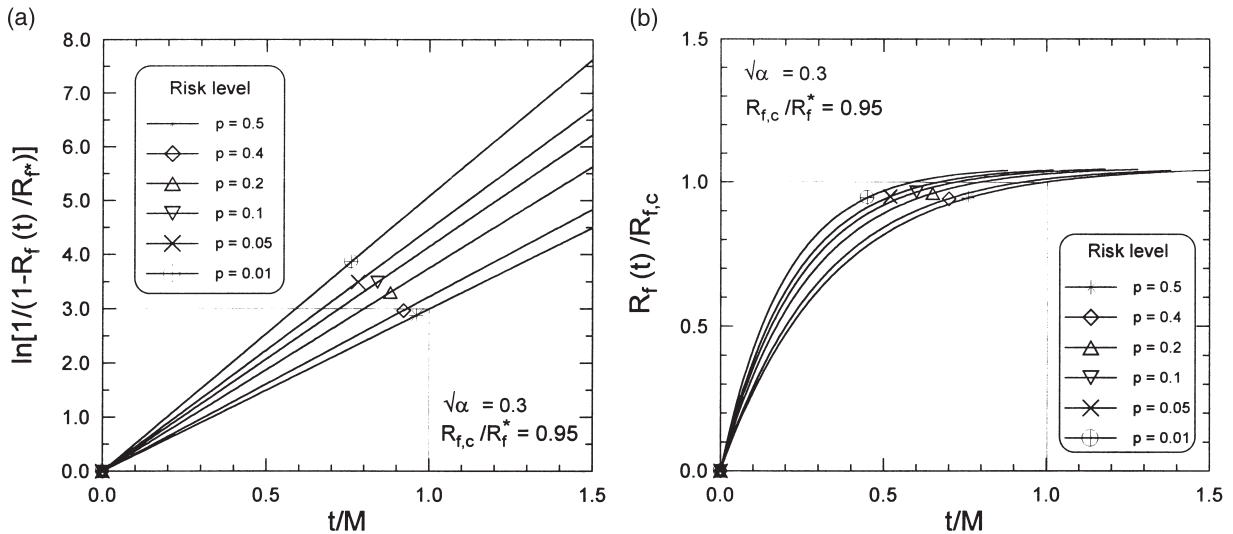


Fig. 4. Reduced random fouling resistance versus reduced time for an exponential model with different values of risk level p and scatter parameter $\sqrt{\alpha}=0.30$: (a) in a transformed y -axis; (b) in a non-transformed y -axis.

3. Thermal performance of a heat exchanger

The thermal performance of a heat exchanger is defined in terms of temperature effectiveness, which is a function of the temperature difference of the hot- and cold-fluid streams. It normally decreases with time due to increased fouling resistance. For the present risk-based thermal analysis of a heat exchanger, we consider a shell-and-tube heat exchanger in a crude oil preheat train. The relevant properties of the exchanger are shown in Table 1.

It should be emphasized that at any time ‘ t ’ corresponding to a targeted risk level p and known

Table 1
Relevant properties for the fluid streams in the heat exchanger

1	Median time ^a , M (days)	100
2	Total heat transfer area of the heat exchanger, A (m ²)	1070
3	Maximum heat transfer duty, \dot{Q}_{\max} (MW)	27.40
4	Number of shell passes, n	3
5	Number of tube passes per shell	2
6	Inlet temperature (cold stream), $T_{c,i}$ (K)	325.78
7	Inlet temperature (hot stream), $T_{h,i}$ (K)	478.00
8	Cold-side mass-flow rate, \dot{m}_c (kg h ⁻¹)	424,922
9	Hot-side mass-flow rate, \dot{m}_h (kg h ⁻¹)	230,600
10	Overall heat transfer coefficient, U_C (W m ⁻² K ⁻¹)	145.66
11	Critical fouling resistance ^b , $R_{f,c}$ (m ² K W ⁻¹)	2.55×10^{-3}
12	Initial outlet temperature (cold stream), $T_{c,o}(0)$ (K)	452.20
13	Initial outlet temperature (hot stream), $T_{h,o}(0)$ (K)	401.70

^a The value of M is not needed for linear, power-law and asymptotic fouling models.

^b For an asymptotic fouling model, $R_{f,c}=0.95R_f^*$.

M and $\sqrt{\alpha}$, the effectiveness of an exchanger with ‘ n ’ shell passes and $2n, 4n, 6n$, etc. tube passes can be expressed as [20]

$$\varepsilon_n(t, p; \sqrt{\alpha}) = \frac{\dot{Q}(t, p; \sqrt{\alpha})}{\dot{Q}_{\max}} = \frac{\{[1 - \varepsilon_1(t, p; \sqrt{\alpha})C_r]/[1 - \varepsilon_1(t, p; \sqrt{\alpha})]\}^{n-1}}{\{[1 - \varepsilon_1(t, p; \sqrt{\alpha})C_r]/[1 - \varepsilon_1(t, p; \sqrt{\alpha})]\}^n - C_r}, \quad (11)$$

where $\varepsilon_1(t, p; \sqrt{\alpha})$ is the effectiveness of a heat exchanger with one shell pass and 2, 4, 6, etc. tube passes; notice that $\varepsilon_1(0, p; \sqrt{\alpha})$ is the effectiveness of the heat exchanger at time $t=0$ when there is no fouling. It is given in terms of the time-dependent number of transfer units, $NTU(t, p; \sqrt{\alpha})$, and the fluid capacitance ratio ($C_r = \dot{C}_{\min}/\dot{C}_{\max}$) as [21]

$$\varepsilon_1(t, p; \sqrt{\alpha}) = 2 / \left\{ 1 + C_r + \frac{1 + \exp[-NTU(t, p; \sqrt{\alpha})(1 + C_r^2)^{1/2}]}{1 - \exp[-NTU(t, p; \sqrt{\alpha})(1 + C_r^2)^{1/2}]} (1 + C_r^2)^{1/2} \right\}. \quad (12)$$

It should be noted that \dot{C}_{\min} is related to the fluid stream which defines the maximum heat transfer rate that will occur in a counter-flow heat exchanger with an infinite area. For example, when ‘max’ belongs to the hot stream and ‘min’ to the cold stream, we get

$$C_r = \frac{T_{h,i} - T_{h,o}(t, p; \sqrt{\alpha})}{T_{c,o}(t, p; \sqrt{\alpha}) - T_{c,i}}. \quad (13)$$

The NTU at any time ‘ t ’ in the above equation is given by

$$NTU(t, p; \sqrt{\alpha}) = U(t, p; \sqrt{\alpha})A/\dot{C}_{\min}, \quad (14)$$

where the time- and risk-dependent overall heat-transfer coefficient can be expressed by considering fouling as an additional resistance to heat transfer as

$$U(t, p; \sqrt{\alpha}) = U_c / [1 + U_c R_f(t, p; \sqrt{\alpha})]. \quad (15)$$

$U(t, p; \sqrt{\alpha})$ and $R_f(t, p; \sqrt{\alpha})$ are the overall heat-transfer coefficient and fouling resistance at any time ‘ t ’ with an associated risk level p and scatter parameter $\sqrt{\alpha}$, respectively; and U_c is the overall heat transfer coefficient under clean conditions. It should also be noted that the outlet, hot- and cold-fluid temperatures are time- and risk-dependent. These temperatures can be easily obtained by calculating their respective enthalpies from the following expression

$$\dot{Q}(t, p; \sqrt{\alpha}) = \dot{m}\Delta H(t, p; \sqrt{\alpha}). \quad (16)$$

After substitution of the hot- and cold-fluid temperatures in the Lee–Kessler equations [22], we get after some simplification [23]

$$\dot{Q}_{\max} = \frac{\dot{m}_h}{\varepsilon_n(t, p; \sqrt{\alpha})} [(a_1 T_{h,i} + a_2 T_{h,i}^2 + a_3 T_{h,i}^3) - (a_1 T_{h,o} + a_2 T_{h,o}^2 + a_3 T_{h,o}^3)], \quad (17)$$

where

$$T_{h,o} = T_{h,o}(t, p; \sqrt{\alpha}). \tag{18}$$

a_1 , a_2 and a_3 are the constants for a fluid stream, which can be determined by using the procedure discussed in API Data Book [22], and $T_{h,i}$, $T_{h,o}$ are the hot-fluid inlet and outlet temperatures, respectively.

A computer program was developed by Sheikh et al. [23] as a part of a general algorithm to study the time- and risk-dependent heat exchanger effectiveness based on a linear random fouling growth model of the exchanger. This program is further extended to incorporate power-law, falling-rate and asymptotic random fouling growth models in determining the heat exchanger’s effectiveness, as well as to study the impact of fouling on the overall heat-transfer coefficient and hot- and cold-fluid outlet temperatures.

4. Results and discussion

The time- and risk-dependent temperature effectiveness of the shell-and-tube heat exchanger discussed in Section 3 are presented in Figs. 5–8 in a reduced coordinate system. In these figures, reduced temperature effectiveness $\varepsilon_n(t, p; \sqrt{\alpha})/\varepsilon_n(0)$ versus reduced time t/M plots for different risk levels p and scatter parameter $\sqrt{\alpha}=0.30$, are plotted for linear, power-law, falling rate and asymptotic fouling-growth models. The overall heat-transfer coefficient under clean condition U_c , the critical fouling resistance $R_{f,c}$, the temperature effectiveness under clean conditions, and other relevant properties are given in Table 1. It is important to mention that for the falling-rate model we have considered $M=100$ days, while for the other models it is not required to assume the value of median time in our calculations. Also for the asymptotic model, we have considered the critical fouling resistance as 95% that of the asymptotic value.

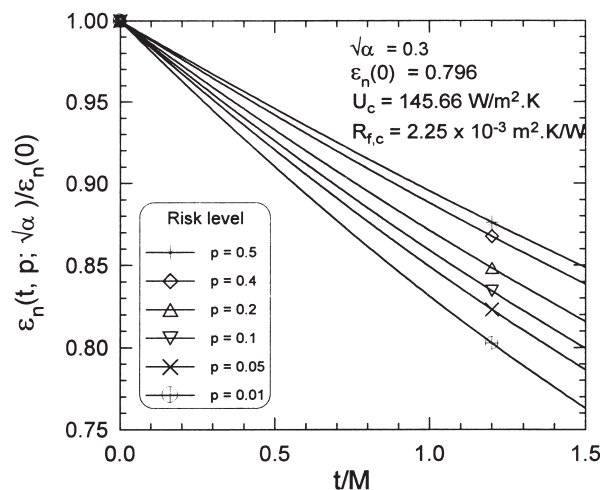


Fig. 5. Reduced temperature effectiveness versus reduced time for a linear random fouling model with different values of risk level p and scatter parameter $\sqrt{\alpha}=0.30$.

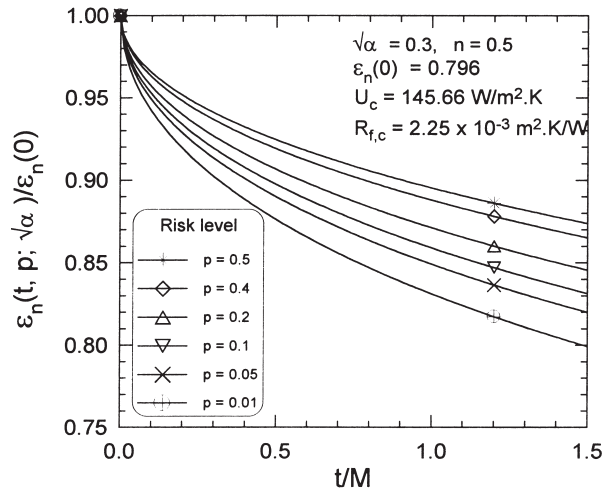


Fig. 6. Reduced temperature effectiveness versus reduced time for a power-law random fouling model with different values of risk level p , scatter parameter $\sqrt{\alpha}=0.30$ and power of the exponent $n=0.50$.

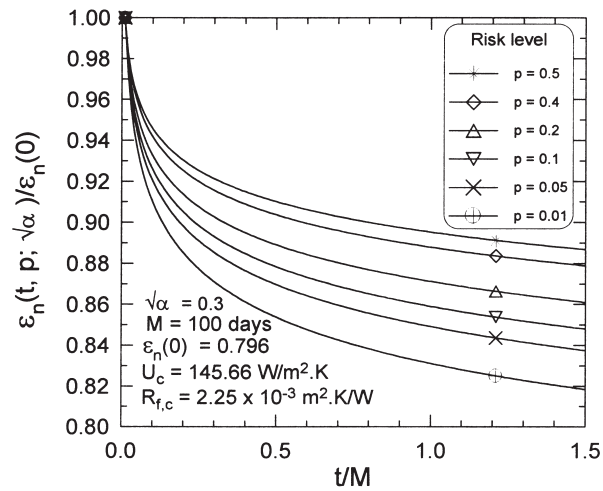


Fig. 7. Reduced temperature effectiveness versus reduced time for a falling-rate random fouling model with different values of risk level p and scatter parameter $\sqrt{\alpha}=0.30$.

As expected, the effectiveness of the heat exchanger degrades significantly with time indicating that, for a low risk level ($p=0.01$), there is about a 17% decrease in effectiveness for a linear fouling model compared with clean conditions when $t/M=1.00$; however, for the deterministic case ($p=0.50$) under the same operating condition, the decrease in effectiveness is about 10%. It should be noted that the behavior of $\varepsilon_n(t, p; \sqrt{\alpha})/\varepsilon_n(0)$ is approximately linear for $t/M \leq 1$. However, for other random fouling growth models, the reduced temperature effectiveness has a non-linear trend, representing somewhat similar behavior to that of the respective underlying random fouling model.

The influence of fouling on the overall heat-transfer coefficient is shown in Figs. 9–12 for all

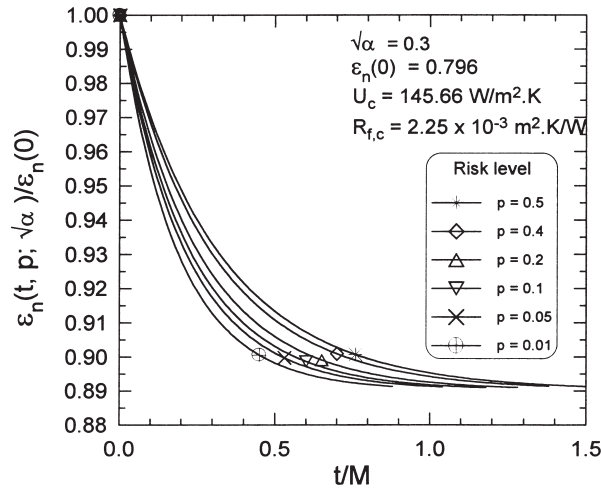


Fig. 8. Reduced temperature effectiveness versus reduced time for an exponential random fouling model with different values of risk level p and scatter parameter $\sqrt{\alpha}=0.30$.

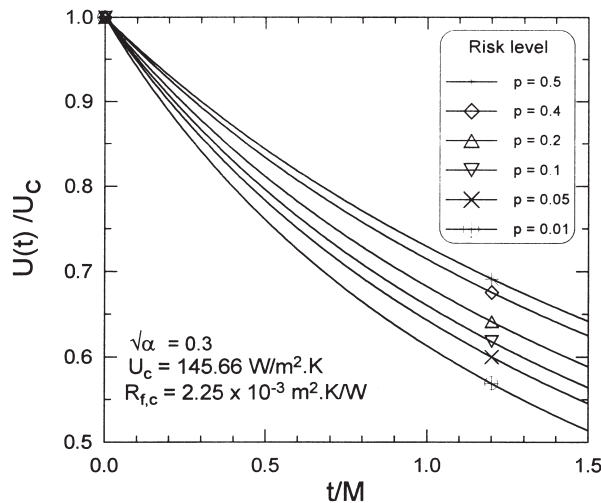


Fig. 9. Reduced overall heat-transfer coefficient versus reduced time for a linear random fouling model with different values of risk level p and scatter parameter $\sqrt{\alpha}=0.30$.

four cases of random fouling growth models. Similar to the temperature effectiveness, the overall heat-transfer coefficient degrades with respect to reduced time. For example, in the case of linear growth of fouling (refer to Fig. 9) when $t/M=1.00$, i.e., when time is equal to the median time, there is about 35% degradation in the value of U compared with the clean condition at $p=0.10$. Similar trends are also noted for the other three fouling growth models; however, it is important to mention that for a fixed value of cleanliness factor $U(t)/U_c$ the time to reach this critical value will be different for different values of risk level. As expected, the deterministic case ($p=0.50$) shows less degradation in the cleanliness factor compared with other risk levels. Similar to the

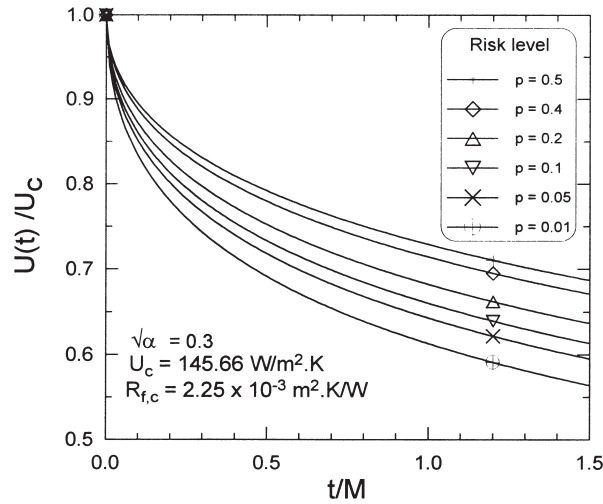


Fig. 10. Reduced overall heat-transfer coefficient versus reduced time for a power-law random fouling model with different values of risk level p , scatter parameter $\sqrt{\alpha}=0.30$ and power of the exponent $n=0.50$.

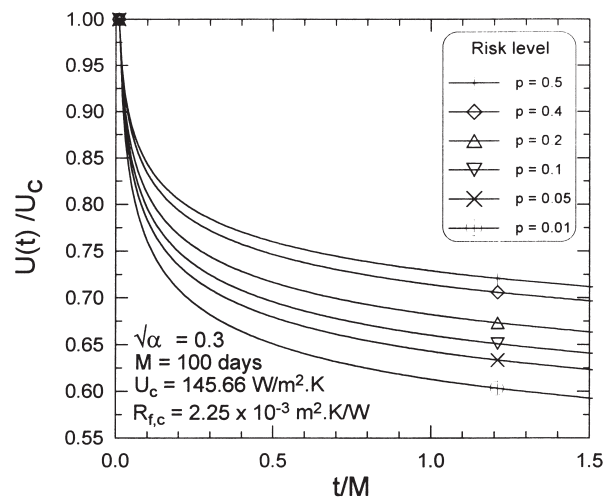


Fig. 11. Reduced overall heat-transfer coefficient versus reduced time for a falling-rate random fouling model with different values of risk level p and scatter parameter $\sqrt{\alpha}=0.30$.

reduced temperature effectiveness curves discussed above, these curves also show trends somewhat similar to that of the respective underlying fouling growth model.

The variations in the reduced hot- and cold-fluid outlet temperatures versus reduced time t/M for different risk levels p and for scatter parameter $\sqrt{\alpha}=0.30$ are shown in Figs. 13–16 for linear, power-law, falling-rate and asymptotic fouling growth models. As one would expect, the figures show that for a low risk level (i.e., high reliability) when compared with the deterministic case, the hot-fluid temperature is high while the cold-fluid outlet temperature is low, indicating that there will be a lower heat transfer rate due to fouling compared with the deterministic case.

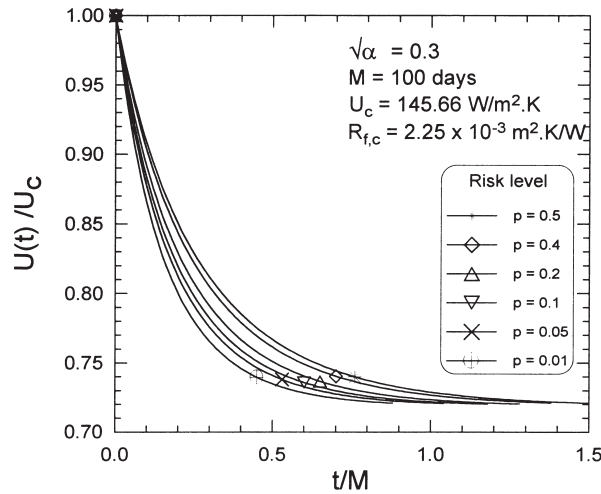


Fig. 12. Reduced overall heat-transfer coefficient versus reduced time for an exponential random fouling model with different values of risk level p and scatter parameter $\sqrt{\alpha}=0.30$.

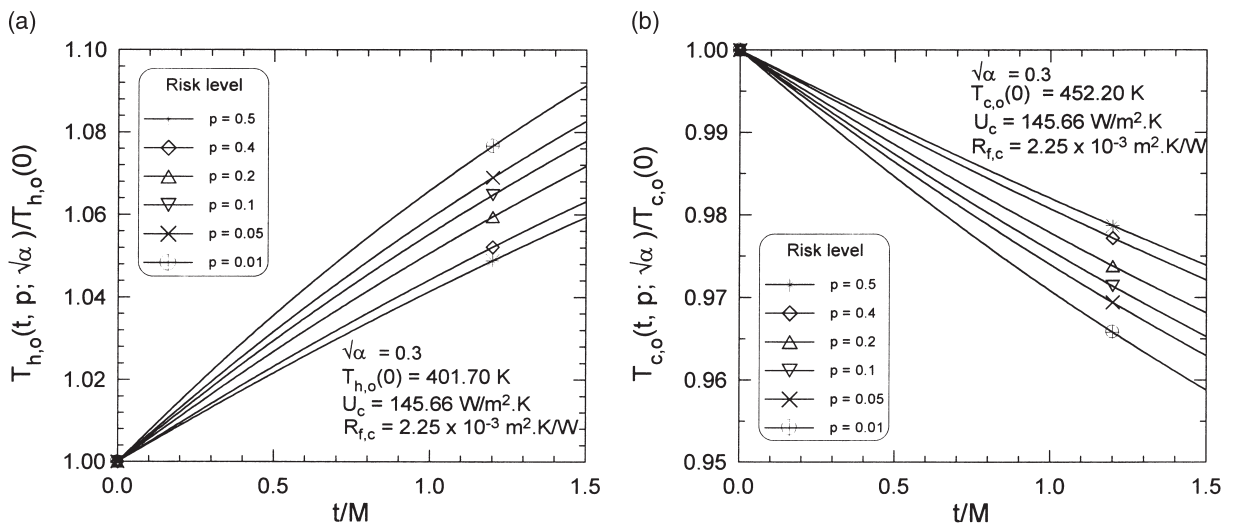


Fig. 13. Reduced outlet temperature versus reduced time for a linear random fouling model with different values of risk level p and scatter parameter $\sqrt{\alpha}=0.30$: (a) hot fluid; and (b) cold fluid.

Similar to the reduced temperature effectiveness and cleanliness factor curves, these curves also show that trends in temperature variations are very similar to that of the respective underlying fouling growth curve (refer to Figs. 1–4) discussed earlier in Section 2.

5. Concluding remarks

A probabilistic approach is discussed to characterize various fouling growth models in terms of the risk level p and scatter in the growth rate of the process $\sqrt{\alpha}$. The models investigated are

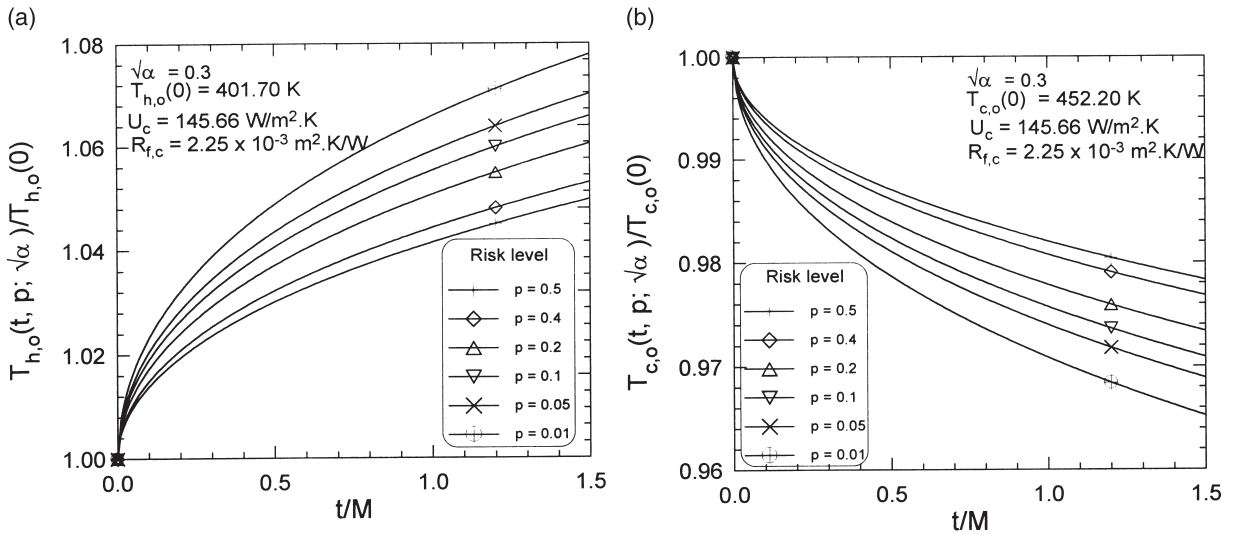


Fig. 14. Reduced outlet temperature versus reduced time for a power-law random fouling model with different values of risk level p , scatter parameter $\sqrt{\alpha}=0.30$ and power of the exponent $n=0.50$: (a) hot fluid; and (b) cold fluid.

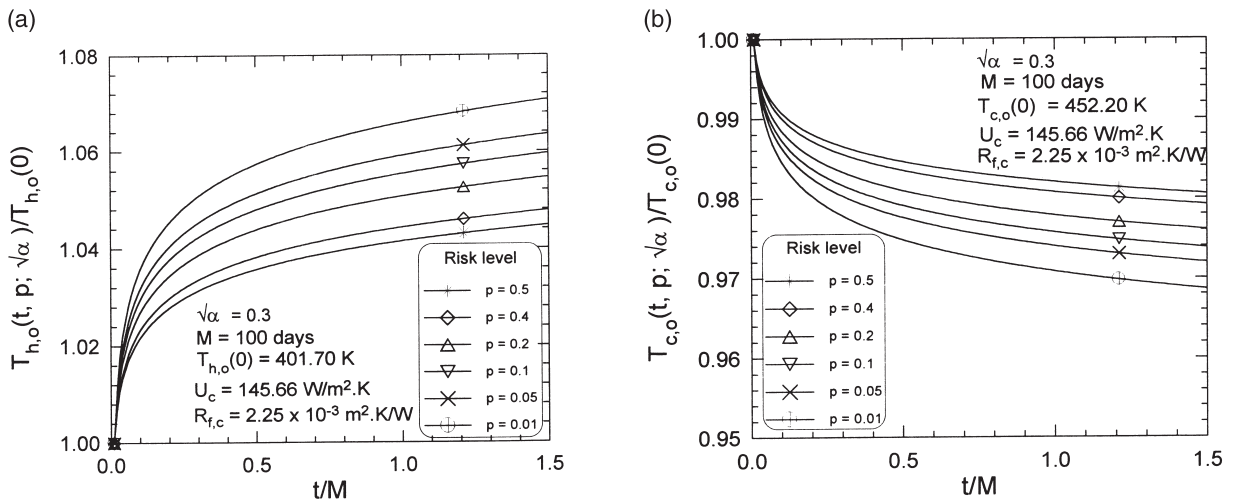


Fig. 15. Reduced outlet temperature versus reduced time for a falling-rate random fouling model with different values of risk level p and scatter parameter $\sqrt{\alpha}$: (a) hot fluid; and (b) cold fluid.

linear, power-law, falling-rate and asymptotic. The non-linear models are transformed into a linear coordinate system so that the probability distribution may be assumed as an alpha distribution in the transformed coordinate system. These random fouling growth models are then considered in the performance evaluation of a shell-and-tube heat exchanger in a crude oil preheat train to demonstrate the influence of risk level and scatter parameter on important thermal parameters of the heat exchangers. All the results are presented in graphical form to demonstrate the impact of risk level in assessing the performance of a heat exchanger. For example, it is clearly demonstrated

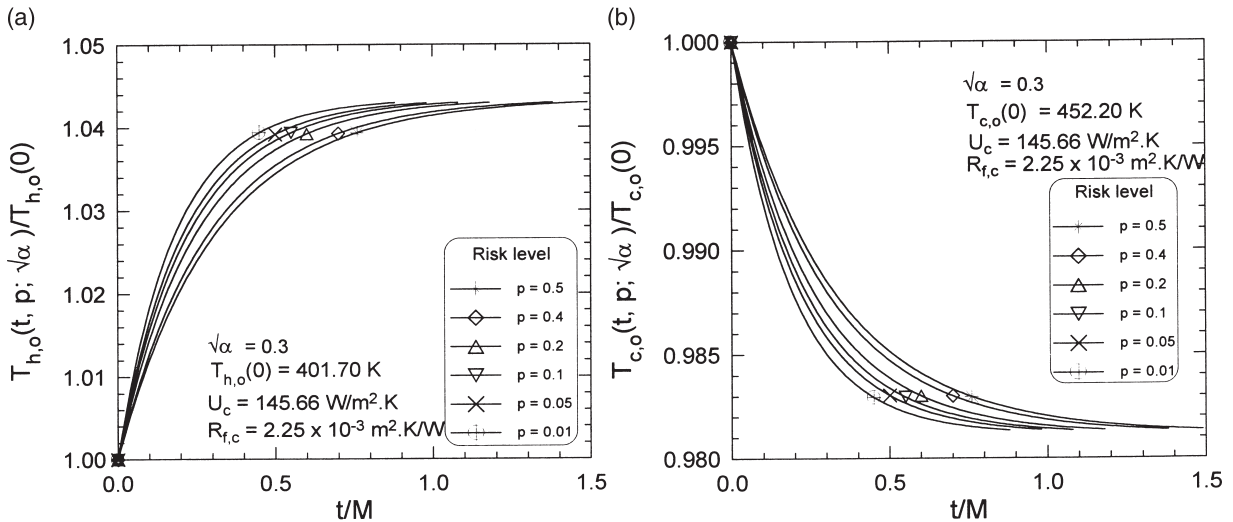


Fig. 16. Reduced outlet temperature versus reduced time for an exponential random fouling model with different values of risk level p and scatter parameter $\sqrt{\alpha}=0.30$: (a) hot fluid; and (b) cold fluid.

that increasing the risk level for a given critical fouling thermal resistance increases the performance characteristics of the exchanger. Although the analysis presented in the paper is applicable to shell-and-tube heat exchangers, the procedure can easily be modified to include other types of heat exchanger such as double pipe, plate-and-frame and other compact heat exchangers.

It is important to emphasize that operating a heat exchanger at a critical risk level is important in some applications such as a heat exchanger network in a refinery. In this regard, an acceptable level of the overall heat-transfer coefficient will primarily govern the cleaning strategy. However, in some situations, heat exchangers are not in a network or in a critical system; here, maintaining the exchanger at a higher reliability level (or at a lower risk level) implies more frequent maintenance intervals, which can often result in increased operation and maintenance costs. It is thus important that, for situations in which the cost of operation and maintenance is an important factor along with the exchanger reliability, the decisions about maintenance can be optimized by developing cost as a function of reliability (or risk level) and then searching for a minimum cost-based solution. This cost-based maintenance strategy is presented in the companion paper.

Acknowledgements

The authors acknowledge the support provided by King Fahd University of Petroleum & Minerals through research project ME/Fouling/176.

References

- [1] Taborek J, Aoki T, Ritter RB, Palen JW, Knudsen JG. Fouling: the major unresolved problem in heat transfer. *Chem Eng Progr* 1972;68(2):59–67.

- [2] Taborek J, Aoki T, Ritter RB, Palen JW, Knudsen JG. Predictive methods for fouling behavior. *Chem Eng Progr* 1972;68(7):69–78.
- [3] Suitor JW, Warner WJ, Ritter RB. The history and status of research in fouling of exchangers in cooling water service. *Can J Chem Eng* 1976;55:374–80.
- [4] Chenoweth JM. Final report of the HTRI/TEMA joint committee to review the fouling section of the TEMA standards. *Heat Transf Eng* 1990;11(1):73–107.
- [5] Bott TR. Fouling of heat exchangers. Amsterdam: Elsevier Science Publishers Ltd, 1995.
- [6] Kern DQ, Seaton RE. A theoretical analysis of thermal surface fouling. *Br Chem Eng* 1959;4(5):258–62.
- [7] Epstein N. Fouling: technical aspects (afterward to fouling in heat exchangers). In: Somerscales EFC, Knudsen JG, editors. Fouling of heat transfer equipment. Washington (DC): Hemisphere, 1981:31–53.
- [8] Al-Ahmad MI, Abdelaleem FA. Scale and fouling problems and its reflection on the performance of industrial thermal processes. In: Proceedings of the 3rd Saudi Engineering Conference. King Saud University Press College of Engineering, Riyadh, Saudi Arabia, Vol. 1, 1991:1–11.
- [9] Zubair SM, Sheikh AK, Shaik MN. A probabilistic approach to the maintenance of heat-transfer equipment subject to fouling. *Energy* 1992;17(8):769–76.
- [10] Zubair SM, Sheikh AK, Budair MO, Badar MA. A maintenance strategy for heat-transfer equipment subject to fouling: a probabilistic approach. *ASME J Heat Transf* 1997;119(3):575–80.
- [11] Sheikh AK, Zubair SM, Younas M, Budair MO. Some remarks on the probabilistic basis for characterizing fouling data. In: Bott TR, Melo LF, Panchal CB, Somerscales EFC, editors. Understanding Heat Exchanger Fouling and Its Mitigation. New York: Begell House, 1999:393–400.
- [12] Hasson D, Avriel M, Resnick W, Rozenman T, Windreich S. Mechanisms of calcium carbonate deposition on heat transfer surfaces. *Ind Eng Chem Fundamentals* 1968;7(1):59–65.
- [13] Andritsos N, Kontopoulou M, Karabelas AJ. Calcium carbonate deposit formation under isothermal conditions. *Can J Chem Eng* 1996;74:911–9.
- [14] Zubair SM, Sheikh AK, Budair MO, Haq MU, Quddus A, Ashiru OA. Statistical aspects of CaCO₃ fouling in AISI 316 stainless steel tubes. *ASME J Heat Transf* 1997;119(3):581–8.
- [15] Khan MS, Zubair SM, Budair MO, Sheikh AK, Quddus A. Fouling resistance model for prediction of CaCO₃ scaling in AISI 316 tubes. *Heat Mass Transf* 1996;32(1-2):73–80.
- [16] Somerscales EFC, Kassemi M. Fouling due to corrosion products formed on a heat-transfer surface. *ASME J Heat Transf* 1987;109(1):267–71.
- [17] Muller-Steinhagen H, Reif F, Epstein N, Watkinson AP. Influence of operating conditions on particulate fouling. *Can J Chem Eng* 1988;66(1):42–50.
- [18] Bansal B, Muller-Steinhagen H. Crystallization fouling in plate heat exchangers. *ASME J Heat Transf* 1993;115(3):584–91.
- [19] Hasson D. Progress in precipitation fouling research — a review. In: Bott TR, Melo LF, Panchal CB, Somerscales EFC, editors. Understanding Heat Exchanger Fouling and Its Mitigation. New York: Begell House, 1999:67–89.
- [20] Jamin B. Exchanger stages solved by graph. *Hydrocarbon Process* 1970;49(7):137–45.
- [21] Kern DQ. Heat exchanger design for fouling service. *Chem Eng Progr* 1966;62(7):51–6.
- [22] Anon. Procedure 7B4.7: alternate computer method for enthalpy of petroleum fractions. API data book — petroleum refining. 4th edition, 1978, 7.133-7.134, American Petroleum Institute, New York
- [23] Sheikh AK, Zubair SM, Haq MU, Budair MO. Reliability-based maintenance strategies for heat exchangers subject to fouling. *ASME J Energy Resourc Technol* 1996;118(4):306–12.